0273-2289/93/3803—0213$04.80

Membrane Oscillator as Chemical Sensor

Part 2: Stable Potential Oscillation of Lipid Membrane across a Micropore

SEIMEI SHA* AND TOYOSAKA MORIIZUMI

Department of Electrical Engineering, Tokyo Institute of Technology, Ookayama, Meguro, Tokyo 152

ABSTRACT

A rhythmic, sustained, stable potential oscillation was reproducibly observed for a lipid membrane supported by a micropore of a thin membrane tip micropipet. Amplitude and period of the oscillation voltage were controlled by changing the pore diameter. The smaller the hole diameter, the smaller the amplitude and the period became. We call this relationship "size effect."

We observed with an optical microscope dynamic behavior of lipids across the oil/water interface, which are formed at a micropore of 2 μm in diameter during self-excited potential oscillation. Periodical movement of a dome-shaped body on the interface is observed, and its expansion and shrinkage are quite synchronous with the potential oscillation.

We also applied this self-excited potential oscillation device as a chemical sensor, and reported the effect of chemical substance added into the water phase as a model for the biological chemoreceptive membrane. The experimental results of microscopic observation show that the sensing system using the micropore can distinguish different chemical substances as well as their concentrations, suggesting its application as a chemical sensor.

*Author to whom all correspondence and reprint requests should be addressed.

SELF-EXCITED POTENTIAL OSCILLATION ACROSS A MICROPORE

Introduction

In biological systems, the brain is continuously fed information received from numerous specialized receptors. These biological sensors convert physical and/or chemical stimuli into nerve impulses through complex cell phenomena.

Since biological systems are very complicated, it has been found profitable to construct artificial systems mimicking the receptor functions, as well as nerve cells, in order to clarify the sensing or signal transmission mechanism of these systems. Moreover, useful devices are expected to appear in this process.

Artificial membranes have been used in various studies of the biological excitation or oscillation mechanism, (*1–4*) but reproducibility has been poor. Yoshikawa and Matsubara reported spontaneous oscillation of electrical potential across a liquid membrane using a U-shaped glass tube 12 mm in diameter (*5*). The reproducibility of their system was, in contrast with previous studies, considerably improved, but oscillation continued only for 2.5 h. Kawakubo and Fukunaga (*6*) improved this system, but oscillation did not continue for more than 5 h. On the other hand, Shimoide et al. used a single micropore in order to support the lipid membrane (*7*). Compared with the liquid-state membrane, the oscillation was not as stable. In this case, however, reproducibility of oscillation was exceedingly improved in comparison to a multipore system, such as the nuclepore membrane (*4*).

We have reported that a rhythmic, sustained, stable potential oscillation was observed for a lipid membrane supported by a thin membrane tip micropipet (TM pipet), and found that stable electrical oscillation could be maintained for more than 120 h using the TM pipet.

In this paper we report that the amplitude and the potential oscillation period can be controlled by changing the pore diameter of the TM pipet, and discuss the possible mechanism of oscillation. Furthermore, the chemical sensing characteristics are described.

Pipet Preparation and Setup for Electrical Measurement

Construction of the TM pipet was accomplished by the method mentioned in Part 1. Five kinds of TM pipets with different hole diameters (8, 3, 2, 0.8, and 0.6 μm) and three kinds of U-shaped glass tubes (10 mm, 2 mm, and 640 μm in diameter) were prepared. In addition, a glass capillary with a hole diameter of 40 μm was prepared by thermally melting the tip of a capillary with an inner diameter of 640 μm. In all, nine kinds of oil/

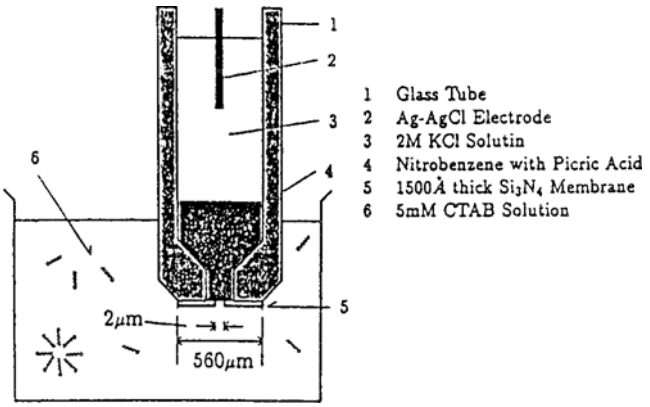

Fig. 1. Illustration of TM pipet structure. Nitrobenzene and 2*M* KCl solution are introduced at the tip of the pipet.

water interfaces were prepared in this experiment. If the hole diameter of the TM pipet was > 10 μm, nitrobenzene could not be supported by the pipet owing to its weight. On the other hand, it is very difficult to reproducibly fabricate a U-shaped glass tube with a μm-order diameter. Therefore, a TM pipet was used to form smaller oil/water interfaces, whereas the U-shaped glass tube was used to form larger interfaces. The inner wall of the TM pipet was made hydrophobic by a standard silanization procedure using dimethyltrichlorosilane. There are two reasons for this silanization. One was to insert oil, such as nitrobenzene, into the pipet easily without leaving a bubble at the tip of the pipet. The other was to stabilize the formation of the lipid membrane at the oil/water interface, which is surrounded by the edge of the micropore. Then, 0.5 μL nitrobenzene including 6.8 m*M* picric acid was introduced at the tip of the pipet with a microsyringe. The remaining cell was filled with a 2*M* KCl solution and a Ag-AgCl electrode was inserted into it. The cross-sectional diagram of the TM pipet is shown in Fig. 1 and the experimental apparatus using the pipet is shown in Fig. 2.

An oil/water interface was formed reproducibly at the hole of the tip simply by dipping the pipet into the water phase with 5 m*M* CTAB (cethyl trimethyl ammonium bromide). When a U-shaped glass tube was used, the formation of the interface was achieved according to the method reported previously (*5*).

In any case, the potential across a liquid membrane consisting of an oil layer (nitrobenzene) between two aqueous phases (5 m*M* CTAB and 2 *M* KCl solution) was recorded by a pen-type recorder through a high-impedance amplifier and/or read out by a computer through an A/D converter. The high-impedance amplifier, batteries, and TM pipet were covered with a copper mesh sheet for electrical shielding. The pipet and water phase were maintained at 25°C throughout the experiment.

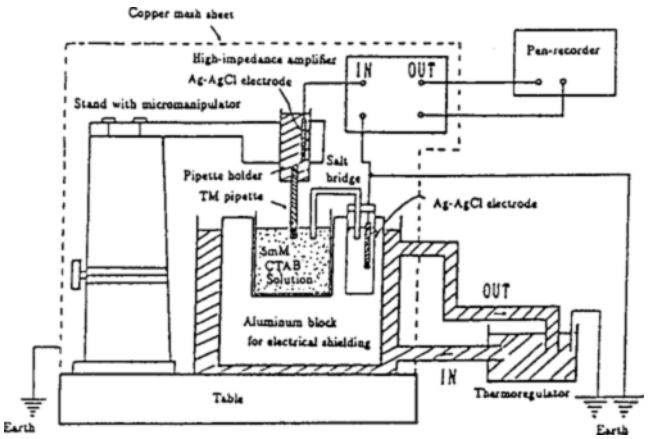

Fig. 2. Diagram of the experimental setup of TM pipet.

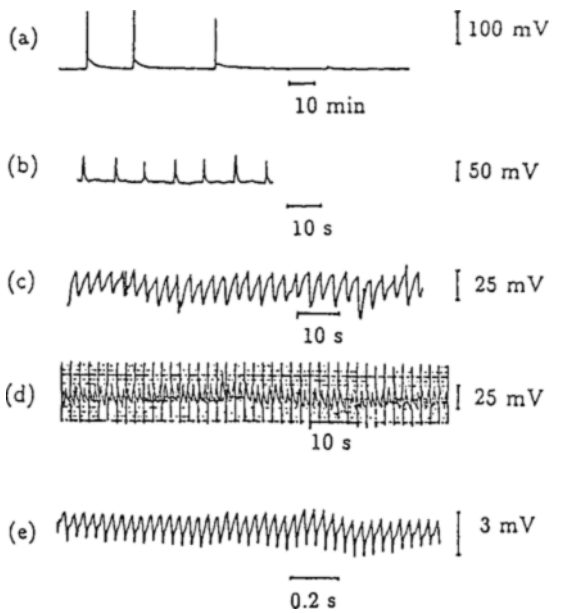

Fig. 3. Typical waveforms of oscillation. The pore diameters are (a) 10 mm (U-cell), (b) 8 μm, (c) 3 μm, (d) 2 μm, and (e) 0.6 μm.

Results and Discussion

Typical tracings of potential oscillation when four diameters of TM pipets and a U-shaped glass tube were used are shown in Fig. 3. In this figure, (a) denotes the tracings when a U-cell of 10 mm in diameter was used. The others, (b), (c), (d), and (e) are the waveforms of oscillation when TM pipets were used with the pore diameters of (b) 8 μm, (c) 3 μm, (d) 2 μm, and (e) 0.6 μm. When the diameter, D, of the oil/water interface was large ((a) and (b)), spike-type oscillation wave shapes were observed.

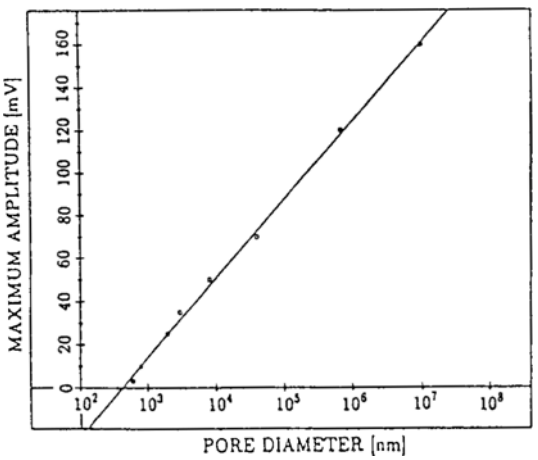

Fig. 4. Relationship between hole diameter and oscillation amplitude.

On the other hand, when the diameter of the interface was small ((c), (d), (e)), the oscillation wave shapes were continuously saw-toothed. The smaller the hole diameter, the smaller the amplitude and the period became.

The relationship between the logarithm of the hole diameter and the oscillation amplitude is shown in Fig. 4. The amplitudes of oscillation had been virtually stable for 120 h when TM pipets were used, but they were often variable when the U-shaped glass tube was used. Their maximum amplitudes are plotted in Fig. 4. The straight line was drawn by fitting the data by the least squares method. This figure shows that the logarithm of the oscillation amplitude is in proportion to log $D^{3.7}$. Consequently, the oscillation amplitude is in proportion to the 1.8 power of the hole area. The correlation coefficient was 0.999.

The relationship between the hole diameter and the oscillation period is shown in Fig. 5. In the case of TM pipets, the oscillation periods were almost constant during the measurement. On the other hand, the oscillation period was not stable when the U-shaped glass tube was used, and the minimum (□) and the maximum (△) periods during the measurement are plotted in the figure. The results can be divided into two parts, as is shown in the figure. The two straight lines in the figure are drawn by fitting the 4 larger points and the 5 smaller points of the minimum period by the least squares method. When the hole diameter, D, is large (>8 μm), the oscillation period is in proportion to $D^{0.6}$. On the other hand, when the hole diameter is small (<8 μm), the oscillation period is in proportion to $D^{2.0}$. In this case, we consider that the oscillation period is in proportion to the area of the oil/water interface at the micropore of the pipet.

When using the smaller pore system, the reproducibility and stability of the oscillation increased remarkably compared with the larger diameter

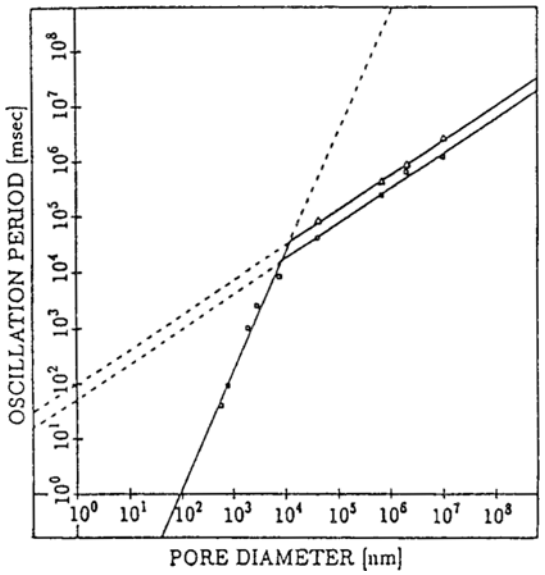

Fig. 5. Relationship between hole diameter and oscillation frequency (□; minimum period, △; maximum period).

system. This suggests that fluctuation of the oscillation phenomenon decreased by limiting the oil/water interface area in which the phase transition of the lipid (*4,5*) probably occurs.

Conclusions

Remarkably stable potential oscillations of a lipid membrane supported by a TM pipet were obtained. The oscillation amplitude and the oscillation period can be controlled by changing the pore diameter of the TM pipet. The oscillation amplitude is in proportion to the 3.7 power of the hole diameter. The oscillation period is in proportion to the micropore area when the pore diameter is small (< 8 μm). On the other hand, the oscillation period is proportional to $D^{0.6}$ when the pore diameter is > 8 μm. The TM pipet system is strongly effective to clarify the mechanism of oscillation phenomena in the biomimetic membrane system.

DYNAMIC BEHAVIOR OF LIPID ACROSS A MICROPORE DURING SELF-EXCITED POTENTIAL OSCILLATION

Introduction

Artificial membranes have been used in various studies of biological excitation or oscillation, (*1–4*) but their real mechanism has not been clarified. One reason for the difficulty in those studies was the poor repro-

ducibility of the oscillation phenomena. Therefore, we have improved the reproducibility and stability of the phenomena through the adoption of a TM pipet (thin membrane tip micropipet) which is fabricated by means of semiconductor technology (*5–7*). In this study, the fluctuation in the oscillation phenomenon was found to be influenced when we decreased the oil/water interface area at which the phase or structure transition of the lipid was supposed to occur (*8*).

Another reason was that the self-excited oscillation phenomenon had been believed impossible to be observed with an optical microscope because it had been thought to be a phenomenon of the order of molecular size. Yoshikawa and Matsubara proposed a hypothesis that the mechanism of self-excited oscillation was the collapse of the lipid monolayer at the oil/water interface (*5*). Although their model was simple and clear, it was not certain that a monolayer was formed at the interface of oil and the aqueous solution of 5 m*M* CTAB (cethyl trimethyl ammonium bromide) whose concentration exceeded the c.m.c. (critical micelle concentration).

In this section, we present a series of microscopic pictures during the potential oscillation taken by a video camera, and report that the self-excited potential oscillation is synchronous with the periodic behavior of a dome-shaped body across the micropore. We will call this body the "dome" hereafter.

Experiments

The supporter of the excitable artificial membrane was fabricated by adopting the method reported by Shimoide et al. (*7*); an Si_3N_4 film of 2000 Å thickness was deposited by LPCVD (low-pressure chemical vapor deposition). A cross-sectional diagram of the cell is shown in Fig. 6. The central part of the Si substrate was removed by EPW (ethylenediamine pylocatechol and water) anisotropic etching. A 2-μm diameter micropore was drilled in the middle of the Si_3N_4 film by electron beam lithography and reactive ion etching. The cell for microscopic observation was fabricated by attaching a glass tube 5 mm in diameter to the periphery of the Si substrate that supported the Si_3N_4 film with a fine pore. A silicone-rubber paste was used for the attachment.

After preparing the cell, 20 μL nitrobenzene mixed with 6.8 m*M* picric acid was introduced from the top of the cell with a microsyringe. The total capacity of the cell was 200 μL. The remaining space of the cell was filled with a 2*M* KCl solution and a spiral Pt electrode was inserted into it. An oil/water interface was formed reproducibly at the hole of the cell by simply dipping the cell into the water phase with 5 m*M* CTAB. One mL ethanol was added into the 2.5-mL water phase. In this condition, the amplitude of self-excited potential oscillation was increased and the dynamic behavior of the dome became easy to observe with a microscope, as is mentioned in the next section.

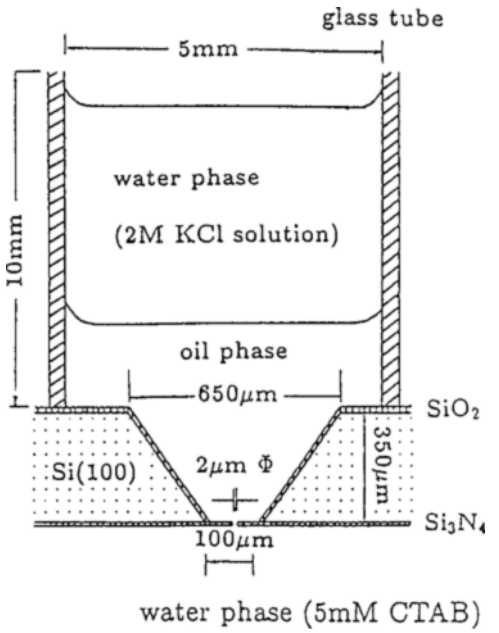

Fig. 6. Cross-sectional diagram of the cell.

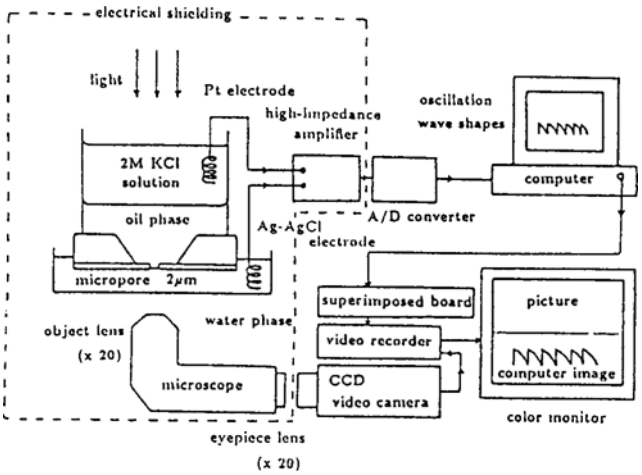

Fig. 7. Diagram of the experimental apparatus.

The experimental apparatus surrounding the cell is shown in Fig. 7. The potential across the three phases of (2*M* KCl solution)/nitrobenzene/(5 m*M* CTAB solution) was read out by a computer through a high-impedance amplifier and an A/D converter. An optical microscope was set under the glass vessel in which the cell was installed. The objective and eyepiece lenses had 20×20 magnification. The microscopic image was monitored by a color TV through a CCD video camera. A regulated DC

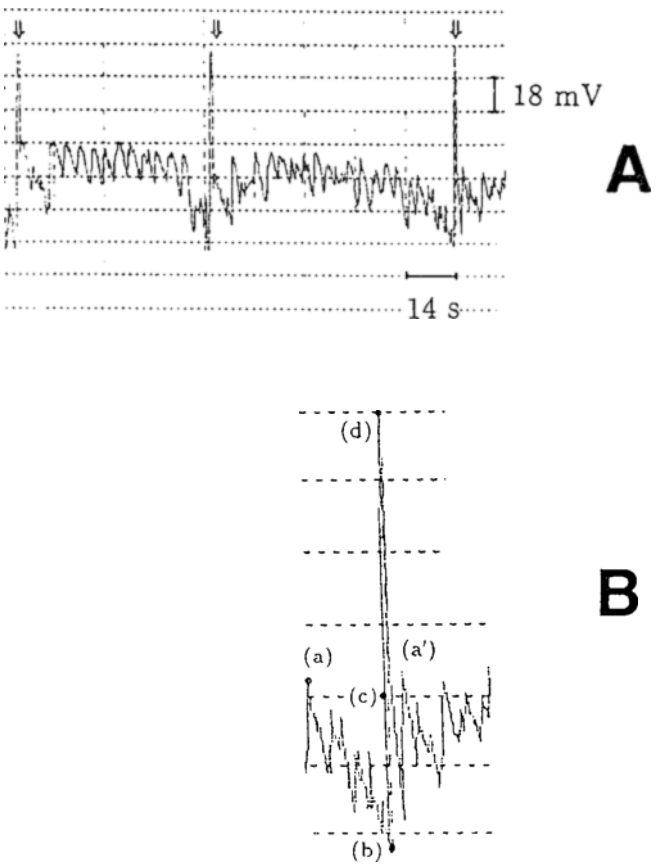

Fig. 8. (a) Typical waveforms of the oscillation. The time scale of the horizontal axis of time and the vertical one of the voltage are 14 s/div and 5 mV/div, respectively. (b) The magnified locus of one spikelike potential oscillation in (a). Points a–d indicate the moment when the photographs were taken (*see* Fig. 4.).

voltage supply was used for the light source of the microscope in order to decrease the noise. The cell and water phases were maintained at 20°C throughout the experiment.

Results

When 2.5 mL of 5 m*M* CTAB was used as a water phase, continuous saw-toothed oscillation was observed, as reported before (*8*). However, when 1 mL of ethanol was added into the water phase, the oscillation waveforms changed, as shown in Fig. 8(a). There were two states of oscillation amplitudes: a smaller amplitude of approx 5 mV and a larger amplitude of approx 30 mV. The spikelike overshoots of this large amplitude were intermittently observed and marked by arrows (↓) in the figure. A

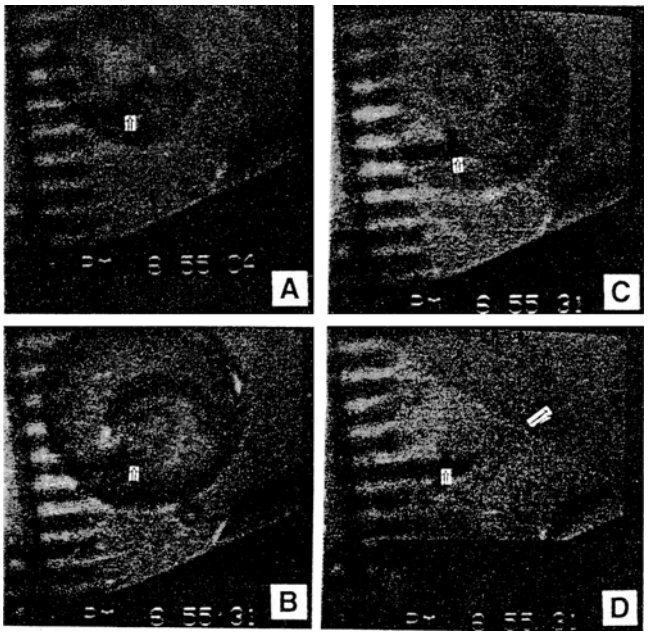

Fig. 9. Behavior of the dome formed in the water phase during the spikelike potential oscillation. The scale in the picture is 5 μm per division. The micropore is indicated by an arrow (↑). The spherelike droplets were sputtered into the oil phase after the burst, as shown by arrows (→): Each photograph of a–d corresponds to points (a)–(d) in Fig. 3(b), respectively.

magnified trace during one period of the spikelike overshoot is shown in Fig. 8(b). Points a–d indicate the moments when the photographs were taken with the microscope and TV display.

The series of photographs taken from the water phase side is shown in Fig. 9. In these pictures, a–d correspond to points a–d in Fig. 8(b), respectively. In each photograph in Fig. 9, the fine hole of 2 μm in diameter is indicated by an arrow (↑). The scale with 5 μm per division is shown on the left side of each photograph. As the 2000-Å -thick Si_3N_4 film is transparent under the light of an optical microscope, the dynamic behavior in both oil and water phases was observed simultaneously.

The sketches of the observed phenomena found in the series of photographs of a–d in Fig. 9 are shown in Fig. 10(a)–(d), respectively. Comparing Figs. 8–10, the phenomena are explained as follows:

a. In the water phase, a dome of 20 μm in diameter was seen. It was found from the microscopic observations at various focusing points that the dome was growing by assembling particles. On the other hand, the droplets (O_1,O_2,O_3) were squeezed out in the oil phase whenever the oscillation with the smaller amplitude showed peaks.

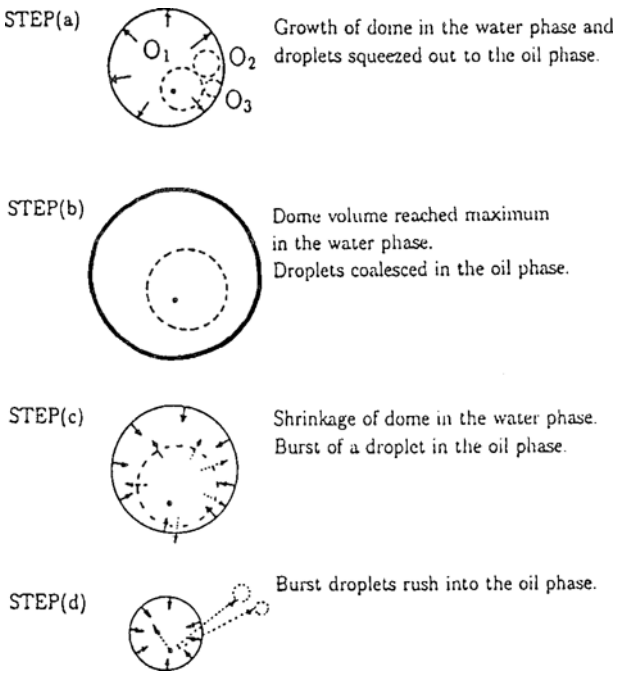

Fig. 10. Sketches of observed phenomena during spikelike potential oscillation. (a)-(d) correspond to the photographs of Fig. 4 a-d. The solid line illustrates the dome in the water phase, and the dashed line the droplets in the oil phase. The observed movements of the dome and the droplets are denoted by arrows.

b. The squeezed droplets coalesced to a larger one. The dome in the water phase grew larger and reached a certain critical size of about 35 μm in diameter at its foot.
c. Soon after step b, the droplet burst in the oil phase, and during the interval between c and d, the dome shrank rapidly. The shrinkage is recognized from the sudden change of the TV image contrast between Figs. 9(b) and (c) at the dome periphery. That change is interpreted resulting from a rapid decrease in dome height. The burst phenomenon occurred within 1 s.
d. After the burst, the volume of the dome became minimum. Until this moment, the contents of the dome went through the micropore and the spherelike droplets rushed into the oil phase, as shown by the arrows (→).

After the burst, the shrunken dome again started to grow. Although the dome did not grow as large as in Fig. 9(a), its diameter began to oscillate at around a certain volume (~ 15 μm). This oscillation was also accompanied by the droplet emission in the oil phase, and was synchronous with the small-amplitude oscillation.

Discussion

No particle was expected to be observed in the bulk of the CTAB solution because the diameter of a micelle was too small to be observed with an optical microscope. However, small particles of submicron sizes were observed moving randomly around but toward the dome. The gathering particles were finally absorbed into the dome and the volume of the dome gradually expanded. Hence, it can be said that the dome was an aggregate of colloidal particles.

Although the process of oscillation mentioned above was the phenomenon that occurred from a to d shown in Fig. 8(b), similar phenomena were observed for each period of continuously sawtoothed potential oscillation with a smaller amplitude, shown in Fig. 8(a). In the latter cases, the average diameter of the dome formed in the water phase was about 15 μm. Since the difference between maximum and minimum of the diameter was smaller than 5 μm (less than one division of the scale shown on the left side of the picture), the movement of the dome could not be captured in still TV pictures. However, on the moving frames of the TV display, the phenomena were quite reproducibly observed, and it can be concluded that the two phenomena of the larger and the smaller amplitudes of oscillations are the same although the amplitude of the potential oscillation and the diameter of the dome were smaller in the sawtoothed oscillation. The phenomenon may have been studied in much more detail if an image processor was adopted in our TV system.

Conclusions

In this study, the dynamic behavior of a lipid across a micropore during the self-excited potential oscillation phenomena was observed by an optical microscope. The series of photographs of the dynamic behavior closely related to the mechanism of self-excited oscillation were taken with a microscope. In the water phase, the domelike lipid aggregate grew, and in the oil phase spherelike droplets were squeezed out. Next, in the water phase, the dome, which had reached a critical volume, shrank, and in the oil phase the droplets burst. The potential change during self-excited oscillation was quite synchronous with the expansion and shrinkage of the domelike lipid aggregate in the water phase.

The present study showed that our experimental setup was suitable for clarifying the mechanism of the oscillation phenomena in an artificially organized membrane system.

SENSING OF CHEMICAL SUBSTANCES

Introduction

It is very attractive to construct devices mimicking the chemical sensing functions of biological receptors. Yoshikawa and Matsubara (*9*) reported

the attempt of creating a taste sensor using the potential oscillation of a U-shaped glass tube 12 mm in diameter. In this case, it took a long time before we would examine the change of oscillation frequency after addition of chemical substance, because the oscillation period is very long (10–30 min, as shown in Fig. 1(a)). Toko and Hayashi (*10*) used lipid membrane as DOPH and examined the effect of taste substance, but the real mechanism of sensing has not been clarified.

We applied the self-excited potential oscillation devise using a micropore as a chemical sensor. As we have explained in the first section, the first advantage of the micropore system was its high reproducibility and its high frequency by limitting the field of oscillation phenomena using semiconductor microfabrication technology. The second advantage of the membrane oscillator using micropore was its handiness. We can use the oscillator as sensor just by dripping the top of the pipet into the water solution.

In this section, the correspondence between the change of oscillation waveshapes and the microscopic pictures of "dome" around the pore is also reported for the first time using our observation system.

Experiments

We applied this self-excited potential oscillation device as a chemical sensor and studied the effect of chemical substance added into the water phase. The effect of taste stimulants added to the water phase with CTAB was investigated as a model for the biological chemoreceptive membranes.

After observing 1 h of stable potential oscillation, various kinds of chemical substances were added into the CTAB solution and change in waveshape responses were examined. Magnesium sulfate, saccharose, citric acid, KCl, and potassium chloride glutamic acid monosodium salt were chosen as bitter, sweet, sour, salty, and umami substances, respectively. When the substances in the water phase were changed, we also changed the nitrobenzene and KCl solution in the TM pipet. In addition, frequency characteristic was also examined by FFT.

We measured the potential change of the TM pipet with 2 μm pore diameter. The reason why a diameter of 2 μm was used is:

1. The smaller the pore diameter, the smaller the amplitude and oscillation frequency became. As we have shown in the figure, when the pore diameter is 2 μm, both oscillation frequency and oscillation amplitude are easy to measure.
2. It is easy to confirm the diameter of 2 μm by an optical microscope.

The experimental setup was the same as in Fig. 7. The observation of behavior of lipids around the pore after adding the chemical substance and the potential measurement were carried out simultaneously.

Results and Discussions

Results of waveshape response are shown in Fig. 11. In this figure, (a) shows the continuous saw-toothed potential oscillation that we have reported previously, and this reproducibility appears before adding chemical substances. (b) shows 20 m*M* of magnesium sulfate (bitter), (c) shows 0.32 m*M* of saccharose (sweet), (d) shows 40 m*M* of citric acid (sour), (e) shows 10 m*M* of KCl (salty), and (f) shows 0.6*M* of potassium chloride glutamic acid monosodium salt (umami substance).

Each measurement was repeated 5 times, and almost the same results were obtained each time, so the reproducibility of the results was confirmed. According to these results, it can be said that we could identify the taste substances just by inserting the pipet into the solution.

As we have mentioned, the advantage of the micropore system was high oscillation frequency and stability compared with the U-shaped glass tube. Thus, it was easy to obtain the frequency spectrum. Fig. 12 shows the time transition of frequency spectrum when the pipet was inserted into the magunesium sulfate as the bitter substance. The sampling period was 55 ms, and the data number was 1024. As are shown in these figures, the basic peak become clear as time passes, and the peak hights of the 2nd, 3rd, 4th, and 5th harmonic waves also increases. Ten minutes after the insertion of the pipet the frequency spectrum became stable. Thus, we decided the frequency characteristics at 10 min after insertion were the characteristics of the solution to examine.

Fig. 13(a) and (b) shows the oscillation waveshapes and frequency spectrum of the 20 m*M* and 40 m*M* of magnesium sulfate, respectively. These two figures show that oscillation frequency and the peak hight of the first harmonic wave was changed by the concentration of the substance in the solution.

For example, the relationship between citric acid concentration and oscillation frequency is shown in Fig. 14. Consequently, it can be said that the oscillation frequency of self-excited potential oscillation of lipids across a micropore changed according to the concentration of the chemical substance in the solution.

In order to examine the mechanism of the change of oscillation waveshapes and oscillation frequency, we observe the behavior of the substances in the solution by optical microscope. We have explained in the second section that the potential oscillation was caused by the expansion and shrinkage of the lipid aggregate gathered around a micropore. The results are shown in Fig. 15. In Fig. 15 (a) shows the condition before adding chemical substance, (b) shows the result after adding 20 m*M* of magnesium sulfate. Small particles formed around the micropore. Here, the scale of 5 μm/division was inserted in each picture. (c) shows the result after adding 0.32*M* of saccharose. In this case, a big round dome was formed around the micropore. (d) shows the result after adding 40 m*M* of

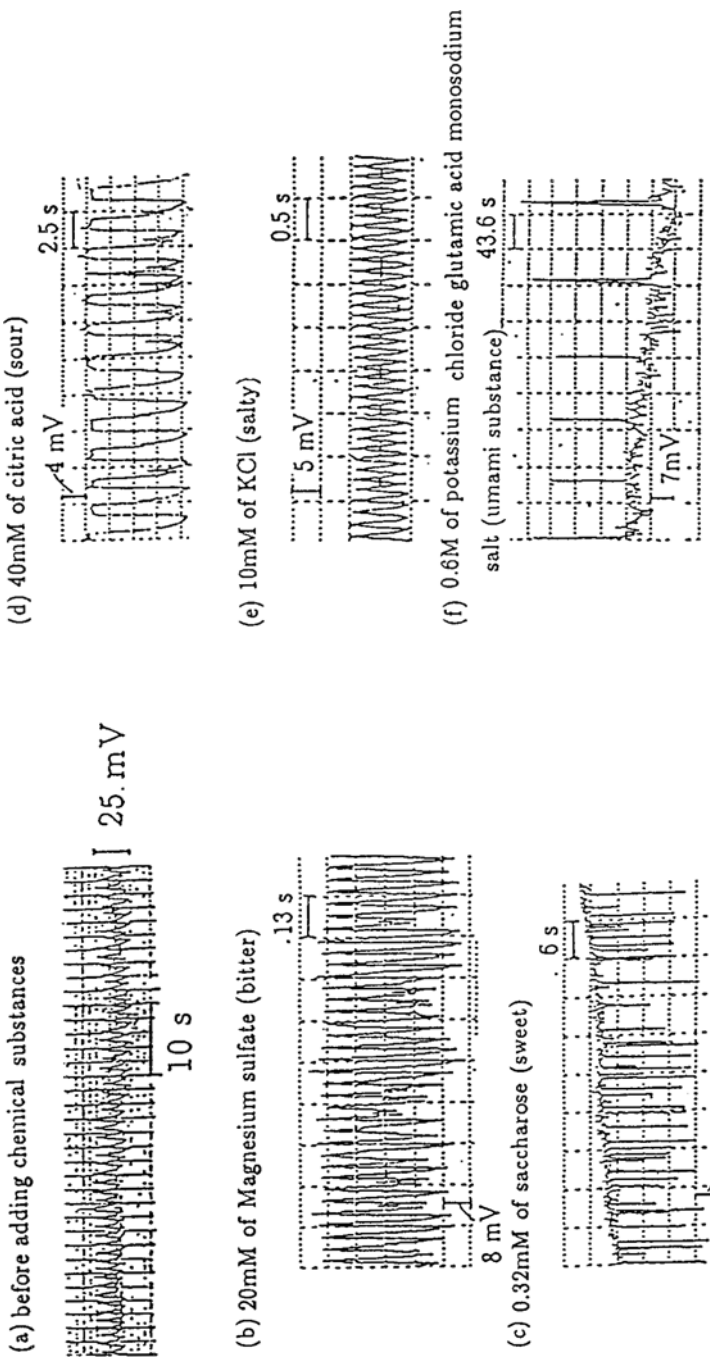

Fig. 11. Results of waveshape response.

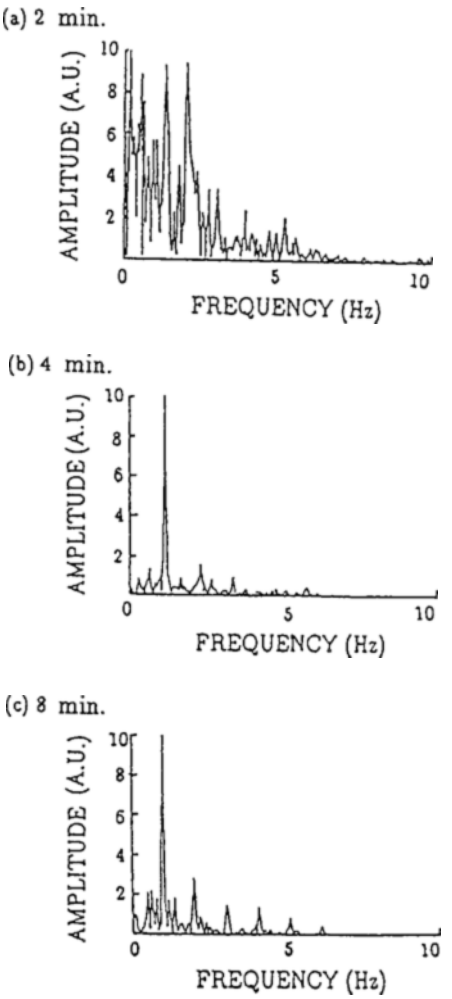

Fig. 12. Time transition of frequency spectrum when the pipet was inserted into the magnesium sulfate.

citric acid, and the aggregation of many round bodies formed around the pore. (e) shows the result of 10 m*M* of KCl. A comparitively small dome was formed around the pore. (f) shows 0.6*M* of glutamic acid monosodium salt. Many white sphere-like bodies gathered and aggregated around the pore. Each photograph shows the condition of the dome in the water phase.

According to the observation using video tape it was found that each dome periodically repeated expansion and shrinkage around the pore. As is shown in these pictures, the dynamic behavior of lipid changes because of the aggregate condition of lipid in the water phase and in the oil phase change.

Consequently, it can be said that the different waveshape responses were caused by the different conditions of aggregation of lipid around the pore.

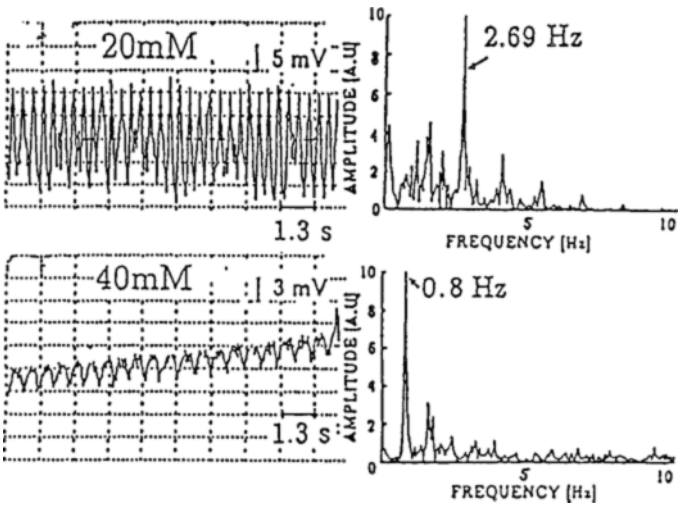

Fig. 13. The oscillation waveshapes and frequency spectrum of 20 m*M* and 40 m*M* magnesium sulfate.

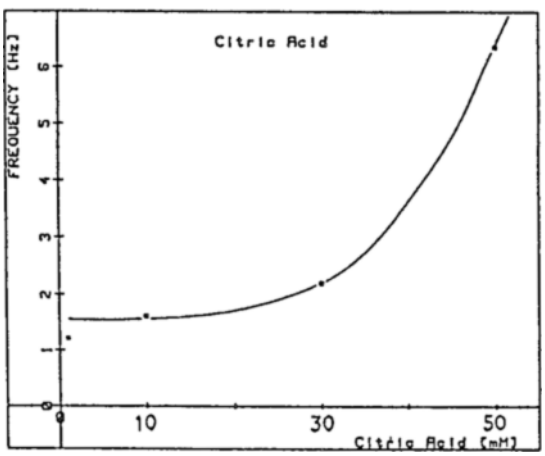

Fig. 14. Relationship between citric acid concentration and oscillation frequency.

Conclusions

In our experiment, we used the dynamic behavior of lipid membrane to form an oil/water interface. As we have mentioned, the real cause of this movement is the marangoni effect—the movement of the oil/water interface. In our results, bitter substances show the highest sensitivity, and sweet substances show the lowest. This relation was very similar to the sensitivity of taste substances of the human body.

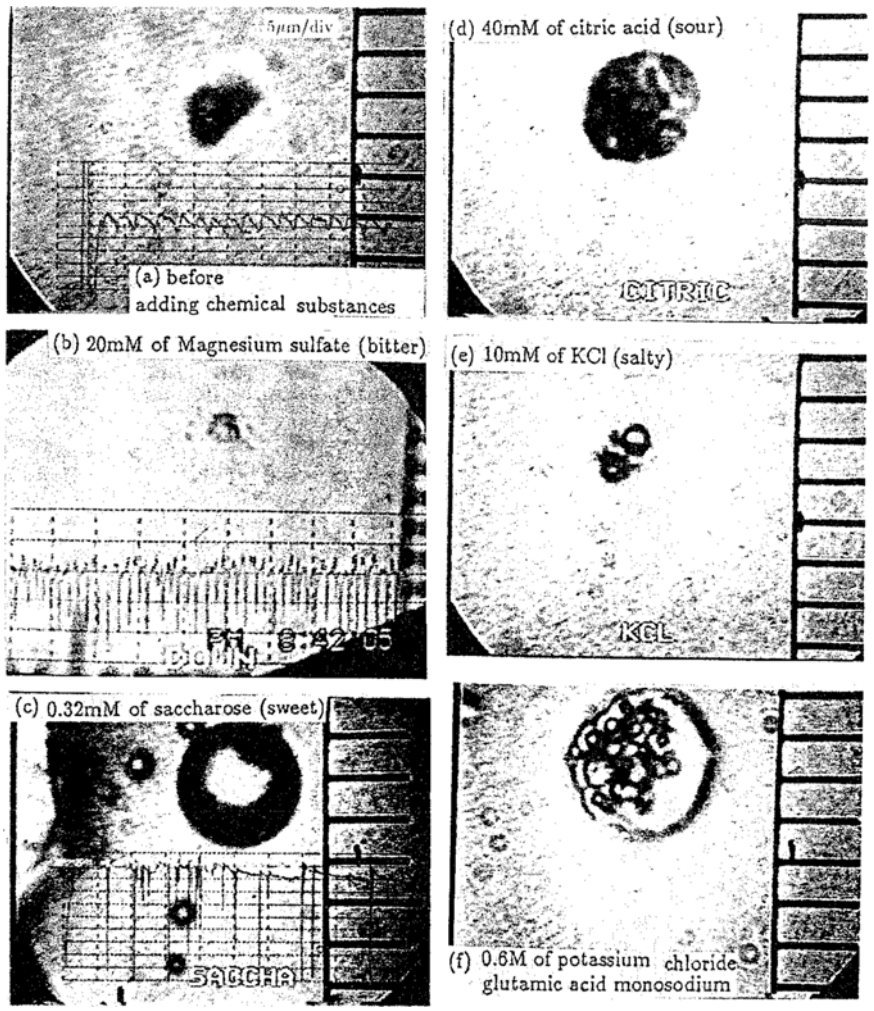

Fig. 15. Behavior of the chemical substances of lipid aggregates in the solution. (a) Before adding chemical substances; (b) 20 m*M* magnesium sulfate (bitter); (c) 0.32 m*M* saccharose (sweet); (d) 40 m*M* citric acid (sour); (e) 10 m*M* KCl (salty); (f) 0.6*M* potassium chloride glutamic acid monosodium.

The results with microscopic observation show that the sensing system using a micropore can distinguish different chemical substances as well as their concentrations, showing its application as a chemical sensor.

It was found that waveshapes' response to chemical substances added to the water phase corresponds to the condition of aggregated lipid around a micropore.

In the future, if we control the micro-''field'' or nano-''field'' much more precisely, we can develop a line-shaped device that is very similar to the human nervous system, or we can develop new biomimetic devices.

REFERENCES

1. Teorel, T. (1959), *J. Gen. Physiol.* **42,** 831.
2. Teorel, T. (1962), *Biophys. J.* **2,** 27.
3. Mueller, P. and Rudin, D. O. (1968), *Nature* 217.
4. Kobatake, Y. (1970), *Physica* **48,** 301.
5. Yoshikawa, K. and Matsubara, Y. (1983), *J. Am. Chem. Soc.* **105,** 5967.
6. Kawakubo, T. and Fukunaga, T. (1988), *Ferroelectrics* **86,** 257.
7. Shimoide, K., Qingde, Z., and Moriizumi, T. (1986), *Jpn. J. Appl. Phys.* **25,** 569.
8. Sha, S., Abatti, P. J., Iko, K., Nakamoto, T., and Moriizumi, T. (1991), *Jpn. J. Appl. Phys.* **30,** L1435.
9. Yoshikawa, K. and Matsubara, Y. (1983), *J. Am. Chem. Soc.* **105,** 5967.
10. Hayashi, K. (1990), *Sensors and Actuators* **B2,** 205.
11. Yokoyama, H., Inoue, T., and Hattori, M. (1990), *10th Symposium on Future Elactron Devices,* October 21 Tokyo, Japan, pp. 115–120.
12. Sha, S., Nakamoto, T., and Moriizumi, T. (1991), *Jpn. J. Appl. Phys.* **30,** L1774.